Study of the Conformational Change of Poly(*N*-isopropylacrylamide)-Grafted Chains in Water with Neutron Reflection: Molecular Weight Dependence at High Grafting Density

H. YIM,[1] M. S. KENT,[1] S. SATIJA,[2] S. MENDEZ,[3] S. S. BALAMURUGAN,[3] S. BALAMURUGAN,[3] G. P. LOPEZ[3]

[1]Department 1851, Sandia National Laboratories, Albuquerque, New Mexico 87185

[2]National Institute of Standards and Technology, Gaithersburg, Maryland 20899

[3]University of New Mexico, Albuquerque, New Mexico 87131

Received 22 October 2003; revised 10 March 2004; accepted 29 March 2004
DOI: 10.1002/polb.20169
Published online in Wiley InterScience (www.interscience.wiley.com).

ABSTRACT: The temperature-dependent conformational change of poly(*N*-isopropylacrylamide) (PNIPAM) brushes in D_2O was investigated as a function of the molecular weight (M) at a high grafting density with neutron reflection. PNIPAM chains with three different M values were grafted at the same high surface density from a gold surface by atom transfer radical polymerization. A significant change in the segment concentration profile was observed for all three samples as the temperature passed through the lower critical solution temperature (~30 °C), in contrast to previous results obtained for samples with much lower surface density. Somewhat surprisingly, the fractional change in the first moment of the segment concentration profile ($\langle z \rangle$) from 20 to 41 °C was weaker with increasing M. This is contrary to the trend for systems involving only van der Waals (VDW) interactions, in which higher M chains experience larger conformational changes with change in solvent quality. Indeed, the M dependence of the first moment of the segment concentration profile for the grafted PNIPAM chains at 20 °C was much weaker than has been reported previously for dense brushes involving only VDW interactions under good solvent conditions. At 20 °C, the form of the segment concentration profile varied systematically with M. A single-layer profile resulted for the highest M, but the profiles became more bilayer in character with decreasing M. At 41 °C, the profiles for all three samples were adequately described by a single dense layer with a smooth transition region to bulk D_2O. The weak dependence of $\langle z \rangle$ on M at 20 °C and the trend from a bilayer profile at lower M to a single-layer profile at higher M appear to be related. These results are interpreted in terms of concentration-dependent segment–segment interactions that result in a weak attraction for high segment densities at 20 °C. © 2004 Wiley Periodicals, Inc. J Polym Sci Part B: Polym Phys 42: 3302–3310, 2004

Keywords: poly-(*N*-isopropylacrylamide); grafted polymers; conformational analysis; neutron reflectivity

INTRODUCTION

Poly(*N*-isopropylacrylamide) (PNIPAM) is one of the most well studied temperature-responsive polymers.[1–4] Free chains of PNIPAM in aqueous solutions exhibit a lower critical solution temperature (LCST) of approximately 30 °C, which is attributed to alterations in the hydrogen-bonding interactions of the amide group.[1,5–7] PNIPAM in various forms has been explored for a variety of applications, including controlled drug delivery,[8,9] solute separation,[10,11] tissue culture substrates[12,13]

Correspondence to: M. S. Kent (E-mail: mskent@sandia.gov)

Journal of Polymer Science: Part B: Polymer Physics, Vol. 42, 3302–3310 (2004)

and controlled adsorption of proteins,[14,15] blood cells,[16] and bacteria.[17] With respect to grafted chains of PNIPAM, many useful applications have been explored. Some of these applications may depend on the magnitude of chain conformational changes, in addition to changes in local interactions. However, little attention has been paid to the detailed dependencies of the conformational changes on the molecular weight (M) and grafting density (σ; chains/Å^2). We have initiated such a study with neutron reflection (NR), which is uniquely suited to addressing this question.

NR provides information about the scattering length density (SLD) distribution normal to the surface, which is directly related to the density and atomic composition. Under the assumption of additivity of volumes, the PNIPAM segment concentration profile [$\phi(z)$] can be calculated from the SLD profile. NR has proved to be a powerful tool for studying the molecular arrangement of polymers at surfaces and interfaces.[18–21] The technique has excellent spatial resolution (~10 Å) normal to the surface. Strong contrast between chemical species can be obtained through deuterium labeling. Other techniques have been used previously to study the transition with temperature for PNIPAM grafted or adsorbed chains. These include surface plasmon resonance,[22] atomic force microscopy (AFM),[23,24] hydrodynamic radius measurements by dynamic light scattering,[25–27] and contact-angle measurements.[22,23,28,29] All provide useful information, but none of these techniques reveal the detailed segment concentration profile.

Previously, Yim et al.[30] used NR to investigate the conformational changes of PNIPAM tethered chains with temperature in D_2O for samples with dry film thicknesses of less than 40 Å. These PNIPAM layers were tethered with either end-functionalized preformed polymers or a chain-transfer free-radical method. The concentration profiles of the PNIPAM brushes were determined in D_2O as a function of temperature and also in deuterated acetone at room temperature. Profiles were obtained in the two solvents to investigate the role of the solvent in mediating interactions. The profiles in D_2O were bilayers, whereas the profiles in acetone were smoothly decaying single-layer profiles. The low segment concentration at the surface in acetone indicated that the surface density of these brushes was quite low. For these low-surface-density brushes, the conformational changes with temperature in D_2O were very subtle. No collapse transition was observed.

More recently, we began a study of the conformational change of PNIPAM brushes synthesized by atom transfer radical polymerization (ATRP).[31] With ATRP, PNIPAM brushes can be prepared with a much higher surface density than that achieved with the other methods in our previous work. For a sample with a dry film thickness of 215 Å, we observed significant changes in the conformation with temperature and reported segment concentration profiles for various values between 20 and 41 °C.[31]

In this work, we report the effect of M on the conformational change of PNIPAM grafted chains with temperature, considering only the states well above and well below the transition temperature. We report results for three samples with the same high σ value but different M values prepared by ATRP. The three samples had dry film thicknesses of 360, 215, and 64 Å and corresponding M values of 71,000, 44,000, and 13,000 g/mol at a surface density of 0.0031 chains/Å^2.[32] Using data for the radii of gyration of free PNIPAM chains in water at 20 °C from Kubota et al.,[33] the reduced surface densities ($\Sigma = \sigma\pi R_g^2$, where R_g is the free-chain radius of gyration) for the three samples were estimated to be 78 (71,000 g/mol), 46 (44,000 g/mol), and 12 (13,000 g/mol) and thus were all well into the overlapping regime.

EXPERIMENTAL

Materials

1-Dodecanethiol, 11-mercapto-1-undecanol, 2-bromopropionyl bromide, CuBr, and 1,4,8,11-tetramethyl-1,4,8,11-tetraazacyclotetradecane (Me_4cyclam) were purchased from Aldrich Chemical Co. *N*-Isopropylacrylamide (NIPAM), D_2O (99.9 atom %), anhydrous dimethylformamide (DMF), and anhydrous tetrahydrofuran were also purchased from Aldrich Chemical. NIPAM was recrystallized from hexane; all other materials were used as received.

Grafting of PNIPAM onto the Gold Surface

The PNIPAM brushes were synthesized by ATRP with CuBr and Me_4Cyclam as a catalyst system. The synthetic procedure is described in detail elsewhere.[22] Thin layers of chromium (30 Å) and gold (110 Å) were sequentially sputtered onto a silicon wafer. The gold-coated wafers were cleaned in a UV/ozone chamber for 20 min

and were then submerged overnight in an ethanol solution containing a mixture of 1-dodecanethiol and 11-mercapto-1-undecanol (10/90 v/v). After an ethanol rinse, the self-assembled monolayers (SAMs) were treated with 2-bromopropionyl bromide (0.1 M) in the presence of triethylamine (0.12 M) for 2–3 min for conversion into a bromo-terminated ester. The initiator-modified samples were placed into a DMF solution containing the NIPAM monomer and CuBr/Me_4cyclam catalyst (0.2 M) and were allowed to react for various periods of time so that different M values could be obtained. Three samples were prepared with dry film thicknesses of 64, 215, and 360 Å, as measured by ellipsometry and NR, with good agreement between the results of the two methods. Because these samples were prepared in the same way and had the same fraction of active sites on the surface in each case, we assumed that the surface density was constant and that the samples varied only in M and, perhaps, polydispersity. The samples were rinsed with DMF and ethanol to terminate the reaction and then were cleaned with deionized water and methanol to remove the unbound polymer.

Instrumentation

The neutron reflectivity measurements were performed on the NG7 reflectometer at the National Institute of Standards and Technology. A fixed wavelength of 4.75 Å was used. Reflectivity data from the protonated PNIPAM layers in deuterated water were obtained as a function of the wavevector ($\mathbf{q} = 4\pi\sin\theta/\lambda$, where θ is the angle of incidence with respect to the plane of the interface and λ is the wavelength) from 20 to 41 °C using a liquid cell described elsewhere.[34] In this geometry, the neutron beam entered and exited through the sides of a thick silicon wafer substrate to impinge on the PNIPAM interface with D_2O. Neutron reflectivity probes the SLD profile normal to the surface, which is determined by the density and atomic composition. The SLD profiles were converted into volume fraction profiles under the assumption of additivity of volumes. The SLD profiles were modeled by a stack of slabs; each slab was assigned an SLD, a thickness, and a roughness described by a Debye–Waller factor. Two approaches were used. In the first approach, the data were analyzed with a small number of unconstrained layers (one or two) to represent the grafted PNIPAM profile. In the second approach, the profile was modeled by a large number of layers (2 Å thick) in which the SLD values were constrained to follow various functional forms, such as a parabola or the sum of two parabolas. The Debye–Waller factor between the 2-Å slabs was fixed at zero in the latter case. To constrain the fits, we determined the thicknesses and SLD values of the Cr, Au, silicon oxide, SAM, and dry PNIPAM films in separate experiments. To accomplish this, three preliminary experiments were performed: a sample containing only the metal films was measured with X-ray reflectivity (XR), a sample containing the metal films and SAM but not PNIPAM was measured in the presence of D_2O in the liquid cell by NR, and the sample with all layers was measured *in vacuo* with NR. The SLD of the SAM layer was obtained in the presence of D_2O to account for any D_2O that penetrated this layer. The reflectivity was calculated from the stack of slabs with the optical matrix method.[18,35] Best fit profiles were determined by minimization of least squares. XR, used to determine the electron density profile normal to the surface,[18] was performed both at Sandia National Labs and at the National Institute of Standards and Technology.

RESULTS AND DISCUSSION

NR data for the 71,000 g/mol PNIPAM sample in D_2O at 20 and 41 °C are shown in Figure 1(a). The data are displayed as the reflectivity $\times$ $\mathbf{q}^4$ to compensate for the $\mathbf{q}^{-4}$ decay due to the Fresnel law. The data are shifted on the y axis for clarity. Large changes in the reflectivity can be observed as a function of temperature for $\mathbf{q} < 0.04$ Å^{-1}, reflecting the change in the PNIPAM segment concentration profile. The reflectivity for $\mathbf{q} > 0.04$ Å^{-1} is dominated by the metal layers and shows little change with temperature. The reflectivity returned to that of the original curve upon a subsequent decrease in the temperature to 20 °C. Good reversibility was obtained for several heating–cooling cycles. The best fit profiles are shown in Figure 1(b). The profiles show that the PNIPAM chains contract upon heating from 20 to 41 °C. To compare the three samples, we determined the first moment ($\langle z \rangle$) of the segment concentration profile as a measure of the average thickness. The first moment of the profile decreases from 269 to 252 Å over this temperature range. Regarding the profile shape, at both temperatures the profile is steplike, with a smooth transition region to bulk D_2O. This indicates that

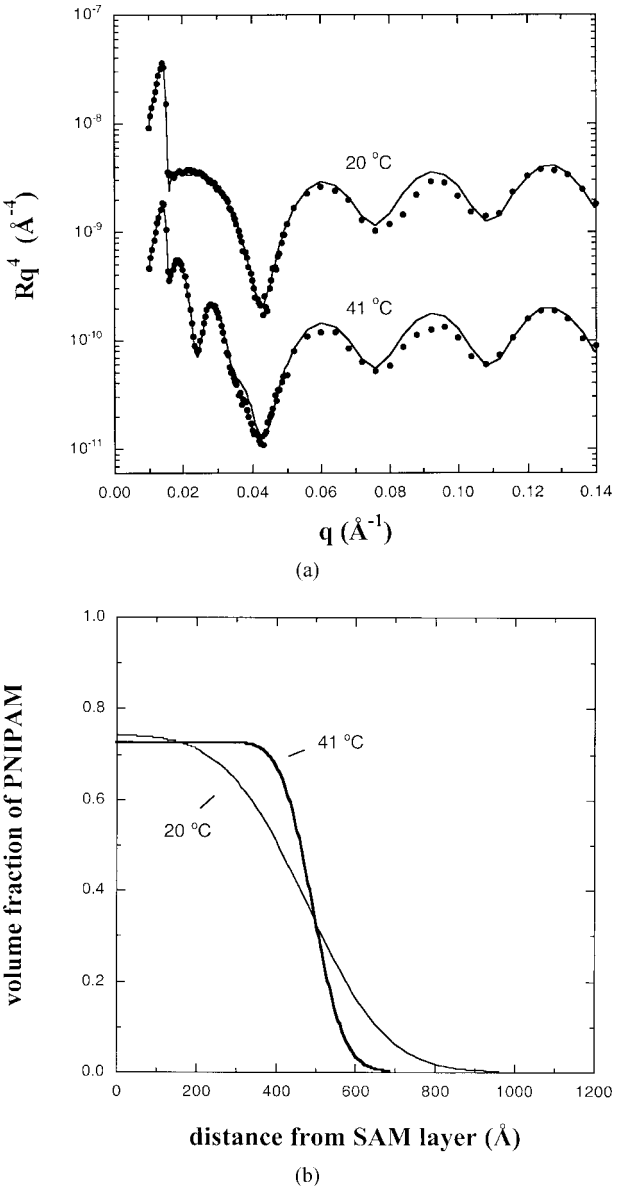

Figure 1. (a) Neutron reflectivity data from the 71,000 g/mol PNIPAM sample at 20 and 41 °C in D_2O. The data at 41 °C have been shifted on the *y* axis for clarity. The error bars are comparable to the size of the symbols at the highest **q** values. The curves through the data correspond to the best fits with model segment concentration profiles (*R* is the reflectivity). (b) Best fit concentration profiles from the 71,000 g/mol PNIPAM sample in D_2O at 20 °C and after heating to 41 °C.

the brush exists in a single dense layer in each case, although the transition region is broader at 20 °C.

Figure 2(a) shows NR data for the 44,000 g/mol PNIPAM sample in D_2O at 20 and 41 °C. Large changes can again be observed over this temperature range for $\mathbf{q} < 0.06$ Å^{-1}. The curves through the data correspond to the segment concentration profiles shown in Figure 2(b). Unlike the 71,000 g/mol sample, a single-layer profile with a smooth transition region to bulk D_2O described by a Debye–Waller factor is not able to precisely describe the data for this sample at 20 °C. Much better agreement with the data can be obtained with a two-slab model, in which the foot of the

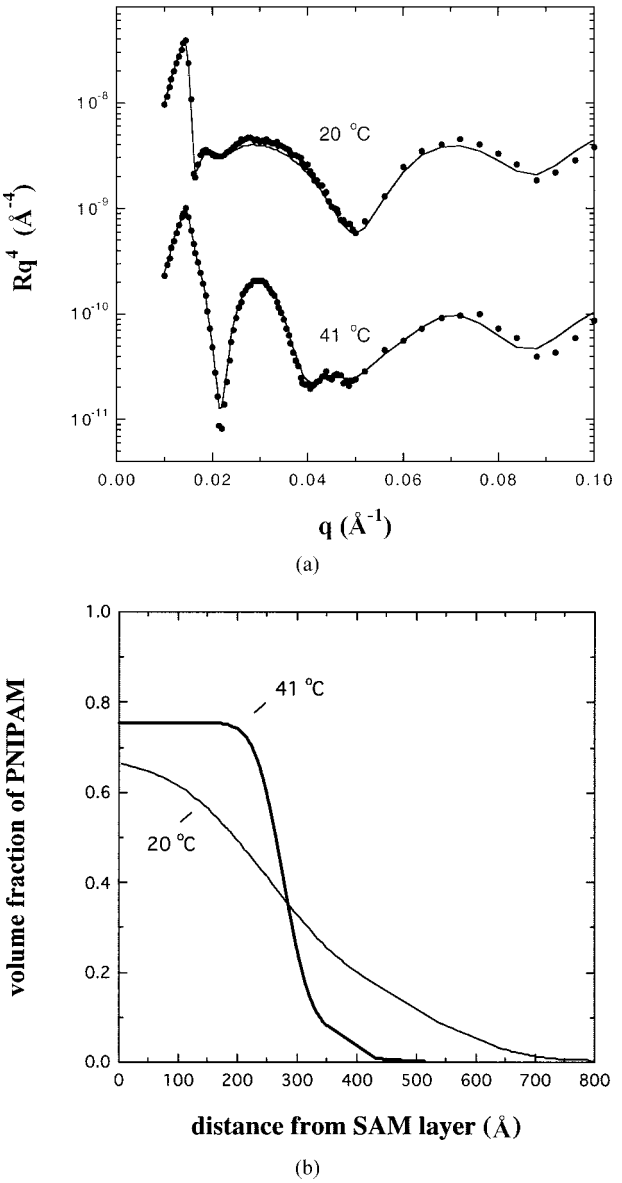

Figure 2. (a) Neutron reflectivity data from the 44,000 g/mol PNIPAM sample at 20 and 41 °C in D_2O. The curves through the data correspond to the best fits with model segment concentration profiles. (b) Best fit concentration profiles from the 44,000 g/mol PNIPAM sample in D_2O at 20 °C and after heating to 41 °C.

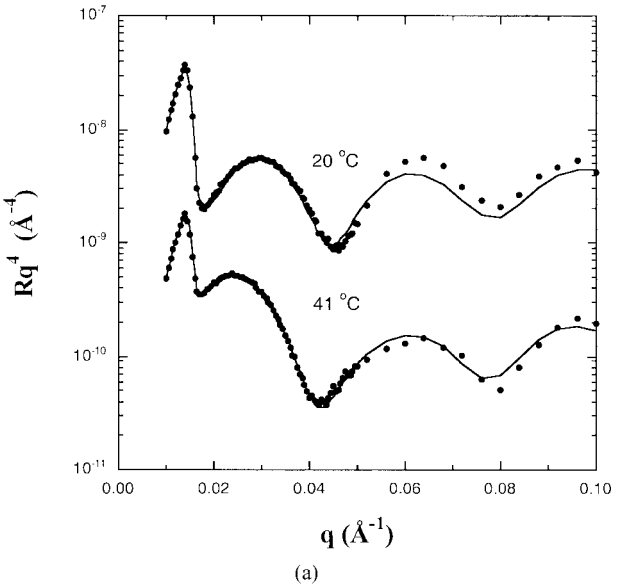

(a)

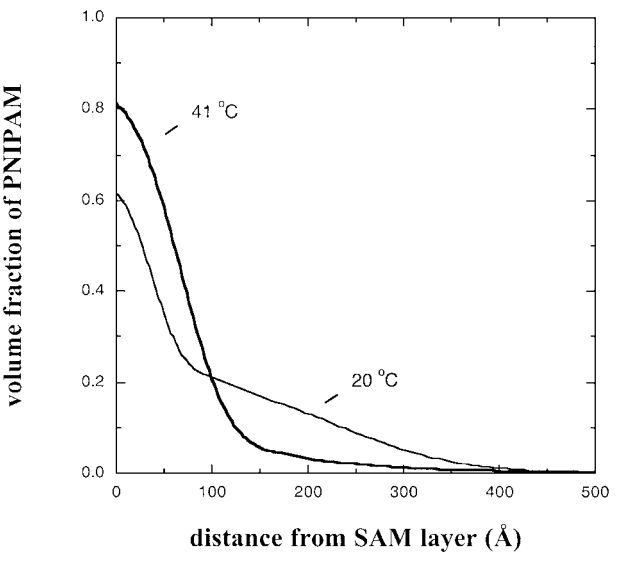

(b)

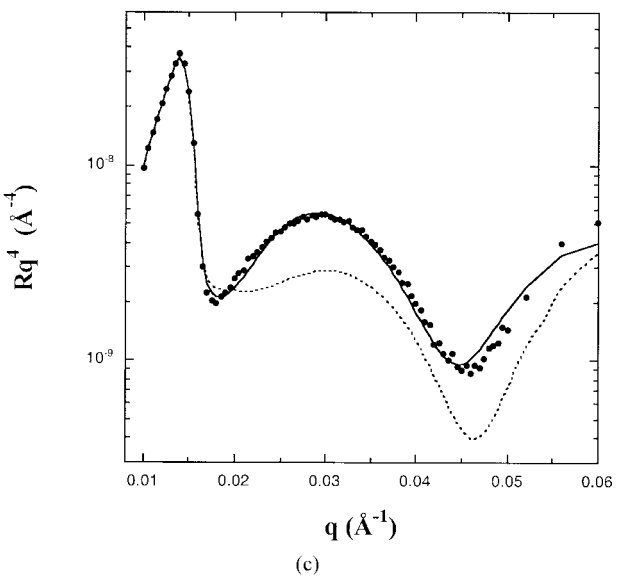

(c)

profile is more pronounced. At 41 °C, the profile is again steplike, with a small transition region. The first moment of $\phi(z)$ decreases from 196 to 149 Å over this temperature range.

Figure 3(a) shows NR data for the 13,000 g/mol PNIPAM sample in D_2O at 20 and 41 °C. For this sample, there was also a significant change in the reflectivity over this temperature range for $\mathbf{q} < 0.06$ Å^{-1}. The curves through the data correspond to the segment concentration profiles shown in Figure 3(b). A distinctly bilayer profile is required to fit the data at 20 °C composed of an approximately 70-Å layer of a high segment concentration at the substrate surface followed by a second layer of a much lower concentration that extends much further into the subphase. The data are not consistent with a single-layer profile with a smooth transition region to bulk D_2O, as for the 71,000 g/mol sample. This is shown in Figure 3(c), which compares the best fits with single-slab and two-slab models with Debye–Waller factors at each interface. The χ^2 value for the best fit with a single-layer profile is 258 compared to 16 for the two-slab profile. As the temperature increases to 41 °C, the profiles in Figure 3(b) reveal that the layer near the substrate surface becomes larger at the expense of the more extended layer. The first moment of $\phi(z)$ decreases from 101 to 64 Å over this temperature range. We note that the profile at 20 °C extends to a distance that is comparable to the theoretical value for full extension of the chains, assuming a monomer length of 3 Å. This is likely due to the fact that the gradient at the solution interface in the model one-dimensional profile includes a contribution from in-plane heterogeneity as well as the actual segment distribution normal to the surface. Polydispersity no doubt also contributes.

The profiles for the three samples at 20 °C are plotted together in Figure 4(a), and those at 41 °C are plotted in Figure 4(b). At 20 °C, the profile becomes more distinctly bilayer with decreasing M, whereas at 41 °C, the shape of the profile varies much less with M.

Figure 3. (a) Neutron reflectivity data from the 13,000 g/mol PNIPAM sample at 20 and 41 °C in D_2O. The curves through the data correspond to the best fits with model segment concentration profiles. (b) Best fit concentration profiles from the 13,000 g/mol PNIPAM sample in D_2O at 20 °C and after heating to 41 °C. (c) Best fits to the data for the 13,000 g/mol PNIPAM sample in D_2O at 20 °C with (- - -) single and (—) two-slab profiles. The error bars are comparable to the size of the symbols at the highest q values.

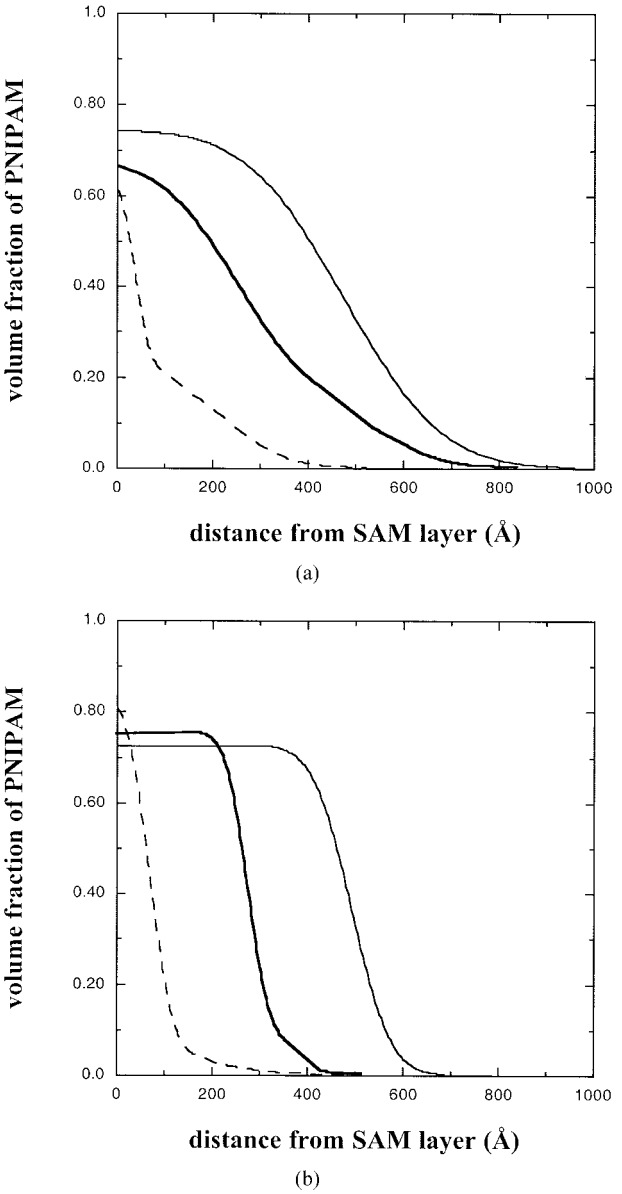

Figure 4. Best fit profiles for the (—) 71,000, (▬) 44,000, and (- - -) 13,000 g/mol samples at (a) 20 and (b) 41 °C.

The first moment of the profile at 20 and 41 °C is plotted versus M in Figure 5. This plot shows that the fractional change of the first moment of the concentration profile with temperature depends strongly on M. As the temperature increases from 20 to 41 °C, the first moment of the concentration profile decreases to 94, 76, and 63% of the value at 20 °C for the 71,000, 44,000, and 13,000 g/mol samples, respectively. The fact that the smallest fractional change in thickness with temperature occurs for the brush with the highest M value is surprising. This arises due to the rather weak dependence of $\langle z \rangle$ on M at 20 °C. If power laws are fit to the data, we obtain $\langle z \rangle = 0.42M^{0.58}$ at 20 °C and $\langle z \rangle = 0.030M^{0.79}$ at 41 °C. We note that the data do not strictly follow a power-law dependence, but rather there is a small systematic deviation in the data from that dependence at both temperatures. Nevertheless two important points can be made. First, the approximate dependence $\langle z \rangle \sim M^{0.58}$ at 20 °C is much weaker than expected for grafted chain systems under good solvent conditions that involve only van der Waals (VDW) interactions, such as polystyrene (PS) in toluene. In the latter case, the dependence is predicted to be $\langle z \rangle \sim M^{0.6}$ for $\Sigma \leq 1$, where the grafted chains do not overlap, and to increase with Σ until the limiting scaling behavior of $\langle z \rangle \sim M$ is reached around $\Sigma \sim 20$.[36] Experimentally, the layer thickness for PS in a good solvent varies as $M^{0.86}$ for $\Sigma = 2$–12,[19] and the layer thickness for poly(dimethylsiloxane) in a good solvent varies as M for $\Sigma = 12$–79.[37] The present data for PNIPAM span a Σ range of 12–78. Thus, the observed dependence is far weaker than expected for good solvent systems involving only VDW interactions, and the amount of chain stretching for the highest M sample is much less than would be expected for a VDW system.[38] Second, the dependence of $\langle z \rangle$ on M is much stronger at 41 °C than at 20 °C. The dependence at 41 °C

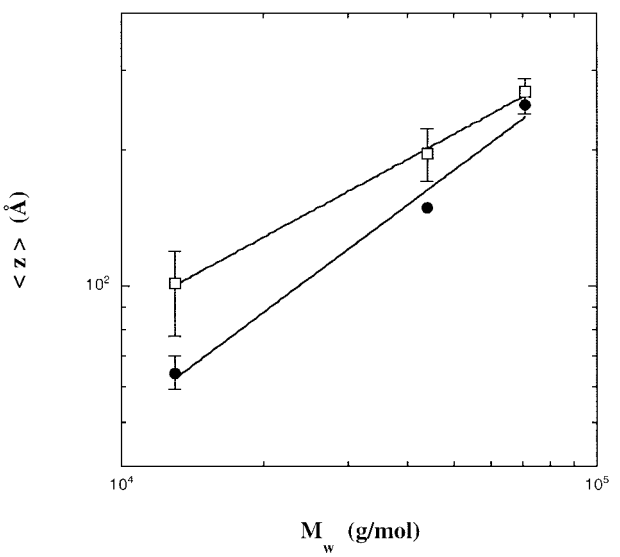

Figure 5. The first moment of the segment concentration profiles versus the weight-average molecular weight (M_w) at (□) 20 and (●) 41 °C. The error bars are comparable to the size of the symbols for the 44,000 and 71,000 g/mol samples at 41 °C.

is closer to the expected limiting scaling behavior of $\langle z \rangle \sim M$. Because the extent of overlap, or Σ, is reduced at 41 °C due to the more contracted R_g under the poorer solvent condition, a dependence somewhat weaker than that for the limiting scaling behavior is reasonable.

The surprisingly weak dependence of $\langle z \rangle$ on M at 20 °C and the trend from a bilayer profile at lower M values to a single-layer profile at higher M values appear to be related. Two possible explanations for this are offered. Both explanations require that the net segment–segment interactions are attractive to some extent at high segment concentrations at 20 °C. This is consistent with the concentration-dependent χ description discussed previously for uncharged water-soluble polymers such as PNIPAM and poly(ethylene oxide) (PEO).[39–46] For such polymers in water, several two-state models have been proposed in which monomers interconvert between hydrophobic and hydrophilic states. These models differ in the presumed physical origin of the two states.[41–45] For example, monomer–monomer contacts may suppress hydrogen bonding between the solvent and monomers[41–43] or cause a difference in the dipole moment due to an internal bond rotation.[44] All of these two-state models result in an effective interaction parameter (χ_{eff}) that is a function of both the monomer volume fraction (ϕ) and the temperature (T). A recent study of bulk phase behavior in PNIPAM/water systems resulted in an empirical expression for $\chi_{eff}(\phi,T)$ that retains a strong concentration dependence even at 20 °C.[46] This expression implies that the segment–segment interactions are attractive at high segment concentrations at 20 °C.

For laterally uniform layers of grafted PNIPAM, the results of the experimentally derived expression for $\chi_{eff}(\phi,T)$ have been examined at 28 °C. This has resulted in the prediction of a vertical phase separation within the brush at high σ values.[39] The bilayer profile reported here for the lower M sample at 20 °C may be consistent with this prediction. However, the M dependence of this effect has not yet been explored theoretically. Therefore, it is not clear if vertical phase separation is expected at lower T for lower M as our data would indicate.

Another possible scenario to explain the trend in the profile shape and the weak dependence of $\langle z \rangle$ on M at 20 °C involves lateral heterogeneity. It is possible that the bilayer at 20 °C for the low-M sample represents a laterally heterogeneous layer and that the layer becomes more uniform with increasing M. In this view, the extra segment density for the higher M sample serves to achieve a more uniform layer, instead of producing additional extension from the surface. Future work involving AFM imaging for the samples with different M values should help to resolve this.

We note that a somewhat similar phenomenon was reported by Szleifer and Carignano[47] even in the absence of concentration-dependent interactions. They treated tethered chains under various solvent conditions with a single-chain mean-field statistical mechanical approach. In theta conditions, they observed lateral heterogeneity and a more bilayer-like distribution at lower Σ values and a steplike profile and a more laterally uniform distribution at higher Σ values (Fig. 34 of ref. 47). They did not report the M dependence of the layer thickness. Their approach treated systems described by the standard concentration-independent Flory χ parameter. Their calculations indicated a more uniform layer under poor solvent conditions as the chains collapsed normal to the surface and spread out laterally to form a relatively uniform carpet. A more homogeneous layer also resulted in good solvent conditions as the chains expanded. Thus, it is possible that the bilayer profile for PNIPAM at 20 °C could be explained by a laterally heterogeneous segment distribution resulting from a sufficiently low Σ value and a concentration-independent χ parameter corresponding to nearly θ conditions. However, Σ is approximately 12 for our lowest M sample, indicating substantial chain overlap. Also, we note that although the dependence of R_g on M for free PNIPAM chains in water at 20 °C ($R_g \sim M^{0.55}$)[33] is somewhat weaker than the dependence for VDW systems under good solvent conditions ($R_g \sim M^{0.60}$ such as for PS in toluene[48]), the observed dependence greater than $R_g \sim M^{0.50}$ indicates a solvent condition substantially better than θ conditions. We do not believe that a solvent condition better than θ can lead to the weak dependence of $\langle z \rangle$ on M observed. Finally, preliminary AFM measurements indicate little change in lateral heterogeneity with temperature. Thus, a concentration-dependent χ_{eff} appears to be a better explanation.

The fact that the profiles for the three samples at 41 °C are more similar in shape than those at 20 °C can be explained by the fact that at 41 °C the segment–segment interactions are much more attractive [or, for $\chi_{eff}(\phi)$, are attractive over a much wider concentration range]. This leads to

more uniform, contracted steplike profiles for all M values.

We note that the conformational changes with temperature reported here are much larger than in our previous study involving PNIPAM chains end-tethered at a low surface density ($<2 \times 10^{-4}$ chains/Å^2) by other methods.[30] The larger conformation change with T is likely due to the much higher surface density in this case. This is in line with the theoretical predictions of Baulin and coworkers[39,40] and more recent numerical self-consistent field calculations.[49] A related experimental result was reported previously by Walldal and Wall.[25] They studied the coil-to-globule transition of PNIPAM adsorbed onto colloidal silica particles with dynamic light scattering. They found that shrinkage of the PNIPAM layer depended on the amount of the adsorbed polymer. When a small amount of polymer was adsorbed onto the particles, a coil-to-globule transition at the LCST did not occur, but instead the contraction of the layer was smooth and gradual with increasing temperature through the LCST. However, when more PNIPAM was adsorbed onto the particles, they observed a distinct transition at the LCST.

CONCLUSIONS

Neutron reflectivity has been used to study the effect of M on the temperature-dependent conformational change of PNIPAM chains grafted at a high density and immersed in D_2O. A significant contraction was observed as the temperature passed through the LCST for all three M values examined. This contrasts with our previous results for samples with much lower surface density. Both the form of the profile and the fractional extent of contraction are strong functions of M. At 20 °C, a single-layer profile was obtained for the highest M sample, but the profiles increased in bilayer character with decreasing M. At 41 °C, the profiles for all three samples were adequately described by a single layer, with a smooth transition region to bulk D_2O. The fractional decrease in the first moment of the concentration profile from 41 to 20 °C was weaker for higher M values. This is in contrast to systems involving only VDW interactions, and arises due to the fact that the M dependence of the layer thickness at 20 °C is far weaker in this system than in VDW systems under good solvent conditions. This latter fact appears to be related to the bilayer profiles observed for the lower M samples at 20 °C. These results are interpreted in terms of concentration-dependent segment–segment interactions, a phenomenological notion derived from the bulk phase behavior of PNIPAM in water and invoked in various two-state models for PNIPAM and PEO.

Sandia is a multiprogram laboratory operated by Sandia Corp., a Lockheed Martin company, for the U.S. Department of Energy under contract DE-AC04-94AL85000. The authors acknowledge the support of the U. S. Department of Commerce National Institute of Standards and Technology in providing the neutron research facilities used in this work and also the support of the Office of Naval Research.

REFERENCES AND NOTES

1. Schild, H. G. Prog Polym Sci 1992, 17, 163.
2. Kubota, K.; Fujishige, S.; Ando, I. J Phys Chem 1990, 94, 5154.
3. Wu, C.; Zhou, S. Macromolecules 1995, 28, 8381.
4. Wang, X.; Qiu, X.; Wu, C. Macromolecules 1998, 31, 2972.
5. Lin, S.-Y.; Chen, K.-S.; Chu, L.-R. Polymer 1999, 40, 2619.
6. Katsumoto, Y.; Tanaka, T.; Sato, H.; Ozaki, Y. J Phys Chem A 2002, 106, 3429.
7. Hirotsu, S.; Yamamoto, I.; Matsuo, A.; Okajim, T.; Furukawa, H.; Yamamoto, T. J Phys Soc Jpn 1995, 64, 2898.
8. Hoffman, A. S. J Controlled Release 1987, 6, 297.
9. Stayton, P. S.; Shimoboji, T.; Long, C.; Chilkoti, A.; Chen, G.; Harris, J. M.; Hoffman, A. S. Nature 1995, 378, 472.
10. Feil, H.; Bae, Y. H.; Jan, F.; Kim, S. W. J Membr Sci 1991, 64, 283.
11. Park, Y. S.; Ito, Y.; Imanishi, Y. Langmuir 1998, 14, 910.
12. Yamada, N.; Okano, T.; Sakai, H.; Karikusa, F.; Sawasaki, Y.; Sakurai, Y. Makromol Chem Rapid Commun 1990, 11, 571.
13. Okano, T.; Yamada, N.; Okuhara, M.; Sakai, H.; Sakurai, Y. Biomaterials 1995, 16, 297.
14. Kawaguchi, H.; Fujimoto, K.; Mizuhara, Y. Colloid Polym Sci 1992, 270, 53.
15. Huber, D. L.; Manginell, R. P.; Samara, M. A.; Kim, B.; Bunker, B. C. Science 2003, 301, 352.
16. Okano, T.; Kikuchi, A.; Sakurai, Y.; Takei, Y.; Ogata, N. J Controlled Release 1995, 36, 125.
17. Ista, L. K.; Perez-Luna, V. H.; Lopez, G. P. Appl Environ Microbiol 1999, 65, 2552.
18. Russell, T. P. Mater Sci Rep 1990, 5, 171.
19. Kent, M. S. Macromol Rapid Commun 2000, 21, 243.

20. Fragento-Cusani, G. J Phys: Condens Matter 2001, 13, 4973.
21. Krueger, S. Curr Opin Colloid Interface Sci 2001, 6, 111.
22. Balamurugan, S.; Mendez, S.; Balamurugan, S. S.; O'Brien, M. J., II; Lopez, G. P. Langmuir 2003, 19, 2545.
23. Kidoaki, S.; Ohya, S.; Nakayama, Y.; Matsuda, T. Langmuir 2001, 17, 2402.
24. Jones, D. M.; Smith, J. R.; Huck, W. T. S.; Alexander, C. Adv Mater 2002, 14, 1130.
25. Walldal, C.; Wall, S. Colloid Polym Sci 2000, 278, 936.
26. Zhu, P. W.; Napper, D. H. J Colloid Interface Sci 1994, 164, 489.
27. Zhu, P. W.; Napper, D. H. Colloids Surf A 1996, 113, 145.
28. Takei, Y.; Aoki, T.; Saui, K.; Ogata, N.; Sakurai, Y.; Okano, T. Macromolecules 1994, 27, 6163.
29. Schmitt, F.-J.; Park, C.; Simon, J.; Ringsdorf, H.; Israelachvili, J. Langmuir 1998, 14, 2838.
30. Yim, H.; Kent, M. S.; Huber, D. L.; Satija, S.; Majewski, J.; Smith, G. S. Macromolecules 2003, 36, 5244.
31. Yim, H.; Kent, M. S.; Mendez, S.; Balamurugan, S.; Balamurugan, S. S.; Lopez, G. P.; Satija, S. Macromolecules 2004, 37, 1994.
32. A PNIPAM sample was polymerized in solution simultaneously with a surface polymerization on a substrate with an SAM containing 90% OH termination, as for these samples. A gel permeation chromatography (GPC) analysis of this sample with PS standards for calibration gave a weight-average molecular weight of 98,500 g/mol and a polydispersity of 2.1. The surface polymerization yielded a dry film thickness of 500 ± 20 Å. The weight-average molecular weight from GPC for the bulk polymerization and the dry film thickness of the surface polymerization corresponded to a surface density of 3.1×10^{-3} chains/Å^2. Under the assumption that the surface density was constant for all polymerizations with 90% OH termination, this value combined with the dry film thickness data yields the M values given in the text.
33. Kubota, K.; Fujishige, S.; Ando, I. Polym J 1990, 22, 15.
34. Satija, S. K.; Majkrzak, C. F.; Russell, T. P.; Sinha, S. K.; Sirota, E. B.; Hughes, G. J. Macromolecules 1990, 23, 3860. The liquid cell used in these experiments was a modification of this original design that allowed the use of circular 4-in. silicon wafers.
35. Styrkas, D.; Doran, S. J.; Gilchrist, V.; Keddie, J. L.; Lu, J. R.; Murphy, E.; Sackin, R.; Su, T.-J.; Tzitzinou, A. In Polymer Surfaces and Interfaces III; Richards, R. W.; Peace, S. K., Eds.; Wiley: New York, 1999.
36. The fact that the limiting scaling behavior of brushes is approached at $\Sigma \sim 20$ has been shown in numerical SCF calculations by Mark Whitmore and his colleagues (Memorial University of Newfoundland) in a private communication.
37. Auroy, P.; Auvray, L.; Leger, L. Phys Rev Lett 1991, 66, 721.
38. Using the relations $R_g = 0.117M^{0.595}$ and $R_g = 0.192M^{0.55}$ for PS in toluene and for PNIPAM in water at 20 °C, respectively, we find almost identical R_g values for M = 71,000 g/mol. However, if the data in Figure 15 of ref. 50 for the layer height of tethered PS chains (M = 60,000 g/mol) in a good solvent, which cover Σ = 1–20, are scaled to M = 71,000 g/mol and extrapolated to Σ = 78, we obtain a value of 590 Å for the first moment, which is much greater than our observed value for PNIPAM in water at 20 °C of 270 Å.
39. Baulin V. A.; Halperin, A. Macromol Theory Simul 2003, 12, 549.
40. Baulin, V. A.; Zhulina, E. B.; Halperin, A. J Chem Phys 2003, 119, 10977.
41. Matsuyama, A.; Tanaka, F. Phys Rev Lett 1990, 65, 341.
42. Bekiranov, S.; Bruinsma, R.; Pincus, P. Phys Rev E 1997, 55, 577.
43. Dormidontova, E. Macromolecules 2002, 35, 987.
44. Karlstrom, G. J Phys Chem 1985, 89, 4962.
45. de Gennes, P.-G. C R Acad Sci Paris II 1991, 117, 313.
46. Afroze, F.; Nies, E.; Berghmans, H. J Mol Struct 2000, 554, 55.
47. Szleifier, I.; Carignano, M. A. Adv Chem Phys 1996, 94, 165.
48. Hugo, Y.; Ueno, N.; Noda, I. Polym J 1983, 15, 367.
49. Mendez, S.; Curro, J. G.; McCoy, J. D. Private communication, 2004.
50. Kent, M. S.; Lee, L. T.; Factor, B. J.; Rondelez, F.; Smith, G. S. J Chem Phys 1995, 103, 2330.